The Korean Journal of Ceramics, 4 [2] 78 - 82 (1998)

Nonstoichiometry (x) of Nuclear Materials UO_{2+x} and $(Ce_yU_{1-y})O_{2+x}$ at High Temperatures as a Function of Oxygen Activity (a_{O_2})

Sun-Ho Kang, Han-Ill Yoo, Han Soo Kim* and Young Woo Lee*

School of Materials Science and Engineering, Seoul National University, Seoul 151-742, Korea
**Korea Atomic Energy Research Institute, P. O. Box 7, Daeduk-Danji, Taejon 305-606, Korea*
(Received October 2, 1997)

The oxygen nonstoichiometry (x) of UO_{2+x} and $(Ce_yU_{1-y})O_{2+x}$ (y=0.05, 0.25) has been measured as a function of oxygen activity (a_{O_2}) at 1000°C by a solid state coulometric titration technique. The results for UO_{2+x} are in a good agreement with literature data and the a_{O_2}-dependence of the nonstoichiometry has been well explained with (2:2:2) cluster model. The equilibrium oxygen activity of $(Ce_yU_{1-y})O_{2+x}$ increases with Ce-content (y) for given nonstoichiometry (x), which is ascribed to the fact that Ce is present as Ce^{3+} and Ce^{4+}, and, therefore, the addition of Ce reduces the oxidation capacity of UO_{2+x}. From the oxygen activity dependence of x in $(Ce_yU_{1-y})O_{2+x}$, the defect structure of $(Ce_yU_{1-y})O_{2+x}$ is discussed.

Key words : UO_{2+x}, $(Ce_yU_{1-y})O_{2+x}$, Nonstoichiometry, Solid state coulometric titration, (2·2·2) cluster

I. Introduction

UO_2-based mixed oxides (MOXs), $(Me_yU_{1-y})O_{2+x}$ (Me=Er, Eu, La, Ce, Pu, Th, etc.), are the most widely used nuclear fuel materials. Metal-to-oxygen ratio, or nonstoichiometry (x) of the MOX fuel is closely related to its physical and chemical properties, e.g., diffusion, creep, electrical and thermal conductivity, release of fission product, and FCCI (Fuel-cladding chemical interaction).[1-5] These properties are very important factors to the preparation of the MOX fuels and to the chemical and physical processes that occur in the MOX fuels during burn-up. The information on the nonstoichiometry (x) as functions of thermodynamic variables, therefore, is crucial in tailoring the material properties of the MOX fuels and predicting the behavior of the fuel in nuclear reactors.

The nonstoichiometry (x) of UO_{2+x} has been extensively studied by thermogravimetry,[5-8] emf-measurement,[9-12] and quenching technique.[13] All of the literature data are in a rather good agreement in magnitude. In defect structure analyses from oxygen activity (a_{O_2}) dependence of x, however, some discrepancy is found especially in intermediate a_{O_2} range where the nonstoichiometry (x) lies between about 0.001 and 0.01.

UO_2-CeO_2 mixed oxide is of technological interest in nuclear reactor because it behaves similarly to UO_2-PuO_2 mixed oxide in the reactor and is also easier to handle. Furthermore, cerium itself is a major fission product that goes into solid solution in the $(U,Pu)O_2$ matrix.[14,15] Some studies on the nonstoichiometry (x) of UO_2-CeO_2 solid solutions have been carried out,[14,16-19] but they are concentrated at temperatures lower than 1000°C and hypo-stoichiometric composition (x<0).

In the present work, the nonstoichiometry (x) of UO_{2+x} and $(Ce_yU_{1-y})O_{2+x}$ (y=0.05 and 0.25) has been measured for hyper-stoichiometric composition (x>0) via solid state coulometric titration. From the oxygen activity dependence of x, the defect structure of UO_{2+x} and Ce-effect on the nonstoichiometry and the defect structure are investigated.

II. Experimental

UO_2 powder was prepared by ammonium uranyl carbonate (AUC) conversion process and CeO_2-UO_2 mixed oxide powder was prepared by mechanical blending of the UO_2 powder with appropriate amount of CeO_2 powder (>99.9%, Aldirich, U.S.A.). Each UO_2 and CeO_2-UO_2 mixed oxide powder was pressed at 300 MPa into green pellets of about 10 mm in diameter and 10 mm in length. Sintering of the green pellets was performed at 1700°C for 4 hours in hydrogen atmosphere. The sintered pellets were then crushed into chips to be used for coulometric titration experiment. Density of each sintered pellet measured by water immersion method was 97.2, 90.5, and 77.5 %TD, respectively.

The nonstoichiometry (x) of UO_{2+x} and $(Ce_yU_{1-y})O_{2+x}$ (y=0.05 and 0.25) was measured by means of solid state coulometric titration with the high-temperature electrochemical cell

$$Pt,(Ce_yU_{1-y})O_{2+x}(a_{O_2}) \,|\, \text{solid electrolyte} \,|\, a_{O_2}^{ref}, Pt \qquad (I)$$

and the experimental cell is schematically shown in Fig. 1. A disk of 8 m/o yttria-stabilized zirconia (8YSZ), 12.5 mm in diameter ×1~1.5 mm thick, was employed as the solid electrolyte. The most critical characteristic of

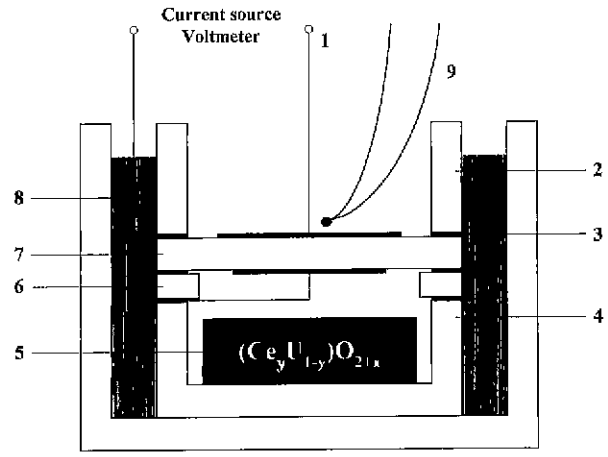

Fig. 1. Schematic diagram of the coulometric titration cell. 1, Pt-lead wire, 2, YSZ ring; 3, Pt foil; 4, alumina cup; 5, specimen; 6, alumina ring; 7, YSZ disk; 8, silicate glass; 9, S-type thermocouple.

an electrochemical cell is that the chamber containing the oxide sample has to be isolated completely from the outer gas atmosphere so that oxygen molecules are supplied to the chamber or removed from it in known amounts only through the solid electrolyte by electrochemical reactions at porous Pt-electrodes. For a complete isolation, silicate glass powder with the composition of 49 wt% SiO_2, 25 wt% BaO, 16 wt% B_2O_3, and 10 wt% Al_2O_3 was used as shown in Fig. 1. At high temperatures above 1000°C, the silicate glass powder melts and provides a gas-tight seal. Details of the preparation of the electrochemical cell have been described elsewhere.[20,21]

Coulometric titration was performed by passing constant currents through the YSZ electrolyte with a d.c. current source (Keithley 224) and measuring open-cell e.m.f. across the electrolyte with a digital multimeter (Keithley 2000). The applied current was the order of 100 μA. The amount of atomic oxygen, ΔN_O, which was removed from or added to the sample chamber can be calculated as

$$\Delta N_O = \frac{I \cdot t}{2F}, \tag{1}$$

where I denotes the applied current for a time duration t, and F the Faraday constant. If the oxygen content in the dead volume of the sample chamber can be neglected as is the case, the change of the oxygen nonstoichiometry, Δx, in $(Ce_yU_{1-y})O_{2\pm x}$ is then given as follows:

$$\Delta x = x - x^* \approx \frac{M}{m} \cdot \Delta N_O = \frac{M \cdot I \cdot t}{2mF} \tag{2}$$

where x^* is the nonstoichiometry at the starting point of coulometric titration, M the molar weight of the specimen, and m the specimen weight. After the current was turned off, the equilibrium oxygen activity over the specimen, a_{O_2}, has been determined via the Nernst equation

$$a_{O_2} = a_{O_2}^{ref} \cdot \exp(-4FE/RT). \tag{3}$$

In Eq. (3), E is the steady state open-circuit e.m.f. across the solid electrolyte, and $a_{O_2}^{ref}$ the oxygen activity of the reference gas flowing outside the titration cell. In the present work, Ar/O_2 or CO_2/CO mixtures were employed as the reference gas, whose oxygen activity, $a_{O_2}^{ref}$ was monitored with a stabilized zirconia oxygen concentration cell.

III. Results and Discussion

1. Nonstoichiometry (x) and defect structure of $UO_{2\pm x}$

In Fig. 2 is shown a titration curve or a nonstoichiometry isotherm, $x(a_{O_2})$, for the system of hyper-stoichiometric UO_{2+x} at 1000°C together with literature data.[5,6,8,10,12] There exists rather good agreement between the present work and the literature data, which had been measured by other methods than coulometric titration, e.g., thermogravimetry, E.M.F. measurement, and quenching technique.

Point defects in UO_{2-x} are known not to exist as isolated defects but to form clusters among them, except for near-stoichiometric compositions ($x \approx 0$). The most frequently adopted defect model in discussing the defect structure of hyper-stoichiometric UO_{2+x} is $(2V_O 2O_i^a 2O_i^b)$ cluster involving oxygen vacancies (V_O) and two different types of interstitial oxygens (O_i^a and O_i^b) proposed by Willis on the basis of neutron diffraction.[22,23] Using the Kröger-Vink notation, the formation of the so-called (2:2:2) cluster is represented by

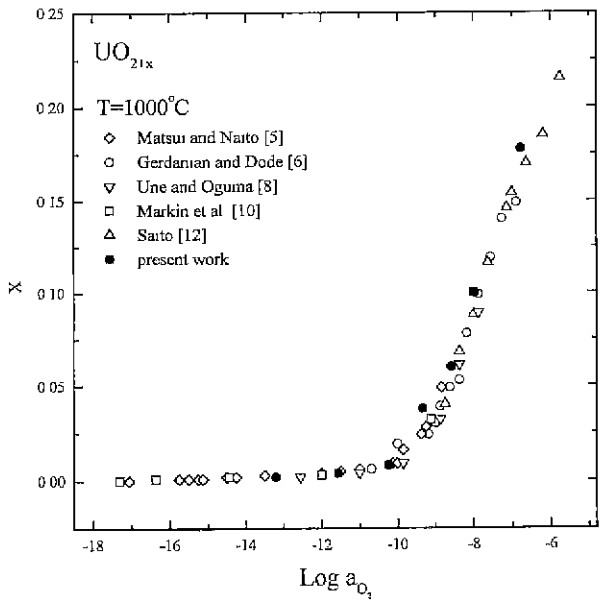

Fig. 2. Nonstoichiometry, x in hyper-stoichiometric UO_{2+x} at 1000°C as a function of oxygen activity (a_{O_2}). Open symbols are from Refs. [5], [6], [8], [10] and [12].

$$2O_O^{\lambda}+O_2(g)+nU_U^{\lambda}=(2V_O2O_i^a2O_i^b)^{n'}+nU_U^{\cdot} \quad :K_{222(n)} \tag{4}$$

where $K_{222(n)}$ and n are the reaction equilibrium constant and the effective charge of the (2:2:2) cluster, respectively. Applying mass action law to Eq. (4) with the assumption that the defects behaves ideally,

$$K_{222(n)}=\frac{[(2V_O2O_i^a2O_i^b)^{n'}]\,[U_U^{\cdot}]^n}{[O_O^x]^2[U_U^{\lambda}]^n a_{O_2}} \tag{5}$$

From the following electroneutrality condition and site balance

$$n[(2V_O2O_i^a2O_i^b)^{n'}]=[U_U^{\cdot}], \tag{6}$$

$$2[(2V_O2O_i^a2O_i^b)^{n'}]=x, \tag{7}$$

log x can be related to log a_{O_2} as follows.

$$\log x=K+\frac{1}{(n+1)}\log a_{O_2}, \tag{8}$$

where

$$K=\frac{1}{(n+1)}\log\left(\frac{2^{n+3}}{n^n}K_{222(n)}\right). \tag{9}$$

In the derivation of Eq. (8), $[O_O^x]$ and $[U_U^x]$ are assumed to be 2 and 1, respectively, due to x<<1. From the slope of a plot of log x versus log a_{O_2}, therefore, the value of n can be calculated and, consequently, charge state of the (2:2:2) cluster can be determined.

Fig. 3 gives log x vs. log a_{O_2} isotherms for the hyper-stoichiometric UO_{2+x} with the data of other workers.[3,6,7,24,25] The slopes for all of the data sets are about 1/5 in low oxygen activity region, and 1/2 in high oxygen activity region. Thus the defect structure of hyper-stoichiometric UO_{2+x} seems to change from a quadruply ionized $(2V_O\ 2O_i^a2O_i^b)''''$ cluster to a singly ionized $(2V_O2O_i^a2O_i^b)'$ cluster with increasing oxygen activity, which means that stronger interaction between (2:2:2) clusters and electron-holes occurs at high a_{O_2}. From the intercepts obtained from the linear regression for the data in Fig. 3, reaction constants for the formation of each (2:2:2) cluster can be calculated from Eq. (9), and the results are listed in Table 1. As temperature increases, the two reaction constants decrease, which means that each oxygen incorporation reaction is exothermic.

As mentioned before briefly, some discrepancy in the analysis of the defect structure of hyper-stoichiometric UO_{2+x} is found among authors especially in the region where $(2V_O2O_i^a2O_i^b)''''$ was concluded to be predominant in the present work. Matsui and Naito[5] reported that

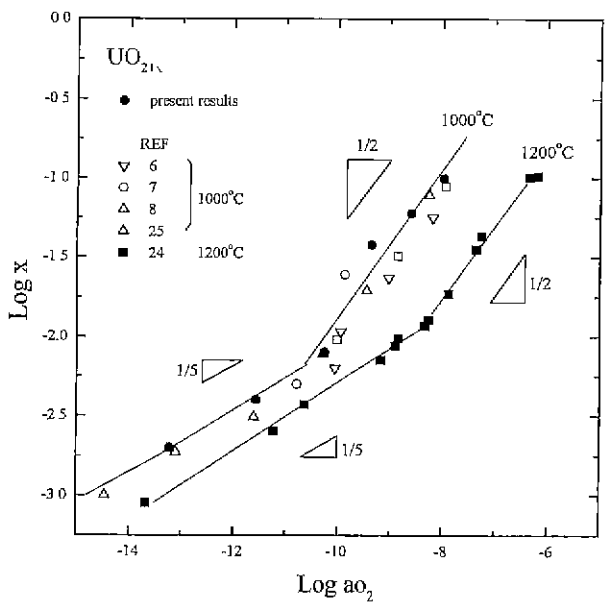

Fig. 3. Log x vs. Log a_{O_2} for hyper-stoichiometric UO_{2+x} at 1000°C and 1200°C. Open symbols at 1000°C are from Refs. [6]-[8] and [23] and the data at 1200°C are from Ref. [14].

the slopes of log x vs. log a_{O_2} plot are 1/2 and 1/12 in the composition range of x>0.006 and 0.003<x<0.006, respectively. The 1/2-slope in high a_{O_2} region (i.e., x>0.006) is the same with the present result and they also interpreted that the 1/2-slope stems from $(2V_O2O_i^a2O_i^b)'$ cluster, but the 1/12-slope in low a_{O_2} region (i.e., 0.003<x<0.006) shows a rather big difference from the present results. To explain the 1/12-slope Matsui and Naito proposed another type of defect model. According to them, as the nonstoichiometry (x) decreases below about 0.006, the defect cluster includes more oxygen vacancies so that $(2V_O\ 2O_i^aO_i^b)$ becomes prevailing, and they explained the 1/12-slope with $(2V_O2O_i^aO_i^b)^{5'}$ model. Markin *et al.*,[10] on the other hand, reported that the log x vs. log has 1/6-slope in the composition range of 0.003<x<0.006.

For more detailed analysis on the defect structure of the hyper-stoichiometric UO_{2+x}, the data on electrical properties, e.g., electrical conductivity and thermoelectric power, are required, which may have the same a_{O_2}-dependence as the nonstoichiometry (x) and can usually be measured more precisely than nonstoichiometry.

2. Nonstoichiometry (x) and defect structure of $(Ce_yU_{1-y})O_{2+x}$

Nonstoichiometry (x) of hyper-stoichiometric (Ce_yU_{1-y})

Table 1. Reactions and their Equilibrium Constants at 1000°C for the Formation of (2:2:2) Cluster Calculated from the Linear Regression of the Present Data at 1000°C and the Literature Data at 1200°C [24] in Fig. 3.

Reactions	Temperature	Reaction equilibrium constant
$2O_O^x+O_2(g)+4U_U^x=(2V_O2O_i^a2O_i^b)''''+4U_U^{\cdot}$	1000°C	Log $K_{222(4)}$=0.0±0.1
	1200°C	Log $K_{222(4)}$=-0.19±0.07
$2O_O^x+O_2(g)+U_U^x=(2V_O2O_i^a2O_i^b)+U_U^{\cdot}$	1000°C	Log $K_{222(1)}$=4±1
	1200°C	Log $K_{222(1)}$=1.9±0.1

O_{2+x} has been measured at 1000°C for cationic compositions of x=0.05 and 0.25 and the results are illustrated in Fig. 4 together with the results for UO_{2+x}. As shown in Fig. 4, the nonstoichiometry isotherms shift towards higher oxygen activity as the Ce-content (y) increases. In other words, the nonstoichiometry (x) decreases at a fixed oxygen activity and the oxidation capacity of $(Ce_yU_{1-y})O_{2+x}$ is reduced with increasing amount of Ce. The shift of the nonstoichiometry isotherms are generally found in Re_2O_3-UO_2 solid solution or $(Re_yU_{1-y})O_{2+x}$, where Re is a rare-earth element having valency of 3, e.g., $(La,U)O_{2+x}$,[26] $(Gd,U)O_{2+x}$,[27,28] and $(Er,U)O_{2+x}$.[4,24,29,30] CeO_{2+x} exists as hypo-stoichiometric oxide (x<0),[31] which means that Ce ion may exist only as Ce^{3+} and Ce^{4+} and the mean valence of Ce ion in CeO_{2+x} is less than 4. The effect of Ce on the nonstoichiometry of UO_{2+x}, therefore, is similar to that of Re and can be understood in terms of the mean valence of the added cation.

In Fig. 5 are represented log x versus log a_{O_2} isotherms for hyper-stoichiometric $(Ce_yU_{1-y})O_{2+x}$ for y=0, 0.05, and 0.25 at 1000°C. For $(Ce_{0.05}U_{0.95})O_{2+x}$, the slopes are 1/5 and 1/2 at low and high a_{O_2}, respectively. The defect structure of hyper-stoichiometric $(Ce_{0.05}U_{0.95})O_{2+x}$, therefore, is concluded to be the same as that of hyper-stoichiometric UO_{2+x}, i.e., a quadruply ionized $(2V_O 2O_i^a O_i^b)''''$ cluster at low a_{O_2} and a singly ionized $(2V_O 2O_i^a O_i^b)'$ cluster at high a_{O_2}. For $(Ce_{0.25}U_{0.75})O_{2+x}$, however, the slopes are different from those of UO_{2+x} and $(Ce_{0.05}U_{0.95})O_{2+x}$: they are 1/2 at low a_{O_2} and 1 at high a_{O_2}. If one could assume that the defect structure of $(Ce_{0.25}U_{0.75})O_{2+x}$ is of the same type as UO_{2+x} and $(Ce_{0.05}U_{0.95})O_{2+x}$, the observed dependencies could be explained with a singly ionized $(2V_O 2O_i^a 2O_i^b)'$ cluster and a neutral $(2V_O 2O_i^a 2O_i^b)^x$ cluster at low and high a_{O_2}, respectively.

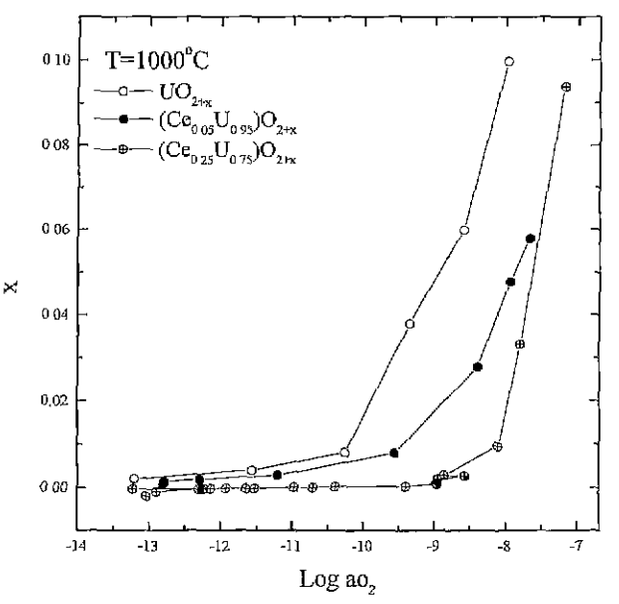

Fig. 4. Nonstoichiometry, x in hyper-stoichiometric $(Ce_yU_{1-y})O_{2+x}$ at 1000°C for the cationic compositions of y=0, 0.05 and 0.25 as a function of oxygen activity.

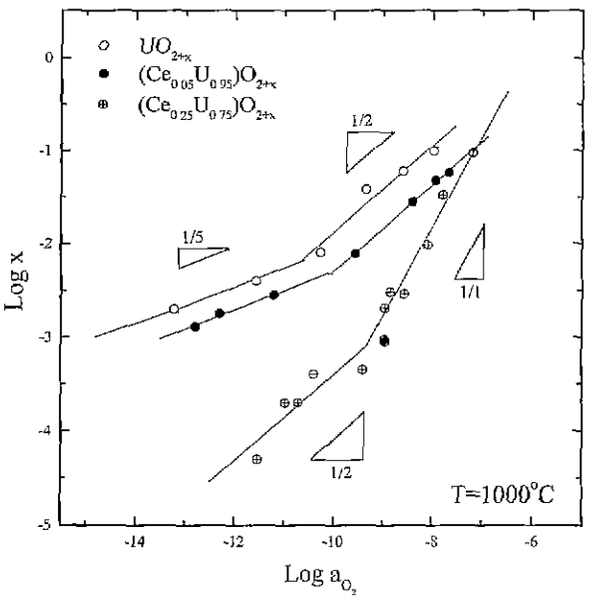

Fig. 5. Log x vs. Log a_{O_2} for hyper-stoichiometric stoichiometric $(Ce_yU_{1-y})O_{2+x}$ at 1000°C for y=0, 0.05 and 0.25.

IV. Conclusions and Summary

The nonstoichiometry (x) of hyper-stoichiometric UO_{2+x}, $(Ce_{0.05}U_{0.96})O_{2+x}$, and $(Ce_{0.25}U_{0.75})O_{2+x}$ has been measured at 1000°C as a function of oxygen activity (a_{O_2}) via solid state coulometric titration.

The log x vs. log a_{O_2} plot for hyper-stoichiometric UO_{2+x} gives straight lines with two different slopes: 1/5 at low a_{O_2} and 1/2 at high a_{O_2}. These dependencies of x on oxygen activity can be explained with a quadruply ionized $(2V_O 2O_i^a O_i^b)''''$ cluster and a singly ionized $(2V_O 2O_i^a O_i^b)'$ cluster at low and high a_{O_2}, respectively.

The nonstoichiometry (x) of hyper-stoichiometric $(Ce_{0.05}U_{0.95})O_{2+x}$ shows the same a_{O_2}-dependence as UO_{2+x}, and it has been concluded that the defect structure does not change at least up to 5 mole% addition of Ce to UO_{2+x}, i.e., a quadruply ionized $(2V_O 2O_i^a 2O_i^b)''''$ cluster at low a_{O_2} and a singly ionized $(2V_O 2O_i^a 2O_i^b)'$ cluster at high a_{O_2}.

For $(Ce_{0.25}U_{0.75})O_{2+x}$, however, the slope at each regime changes : 1/2 at low a_{O_2} regime and 1 at high a_{O_2} regime. This indicates the major defect type is different from that of UO_{2+x} and $(Ce_{0.05}U_{0.96})O_{2+x}$. If $(Ce_{0.25}U_{0.75})O_{2+x}$ is assumed to have the same defect structure as UO_{2+x}, the observed slopes can be explained with a singly ionized $(2V_O 2O_i^a 2O_i^b)'$ cluster at low a_{O_2} regime and a neutral $(2V_O 2O_i^a 2O_i^b)^x$ cluster at high a_{O_2} regime.

References

1. H. Matzke, in Nonstoichiometric Oxides, Ch. 4, Edited by O. T. Sorø nnsen, Academic Press (1981).
2. F. Schmitz and M. Fock, "Diffusion of heavy elements in nuclear fuels: actinides in UO_2", *J. Nucl. Mater.* **17**, 259-

269 (1965).
3. S. Iida, "Electrical Properties of Nonstoichiometric Uranium Dioxide", *Jap. J. Appl. Phys.* **4**, 833-838 (1965).
4. H. S. Kim, "A Study on Themodynamic Properties and Defect Structures of $U_{1-y}Er_yO_{2+x}$ Solid Solutions", Ph. D. Thesis, KAIST, 1995.
5. T. Matsui and K. Naito, "Oxygen Potentials of UO_{2+x} and $(Th_{1-y}U_y)O_{2+x}$", *J. Nucl. Mater* **132**, 212-221 (1985).
6. P. Gerdanian and M. Dode, "Etude Thermodynamique des Oxydes UO_{2+x}", *J. Chim. Physique.* **62**, 171-184 (1965).
7. K. Hagemark and M. Broli, "Equilibrium Oxygen Pressure over the Nonstoichiometric Uranium Oxides UO_{2-x} and U_3O_{8-z} at Higher Temperatures", *J. Inorg. Nucl. Chem.* **28**, 2837-2850 (1966)
8. K. Une and M. Oguma, "Oxygen Potentials of $(U,Gd)O_{2+x}$ Solid Solutions in the Temperature Range 1000-1500°C", *J. Nucl. Mater.* **115**, 84-90 (1983).
9. K. Kiukkola, "High-Temperature Electrochemical Study of Uranium Oxides in the UO_2-U_3O_8 Region", *Acta. Chem. Scand.* **16**[2], 327-345 (1962).
10. T. L. Markin, V. J. Wheeler and R. J. Bones, "High Temperature Thermodynamic Data for $UO_{2\pm x}$", *J Inorg. Nucl. Chem.* **30**, 807-817 (1968).
11. S. Aronson and J. Belle, "Nonstoichiometry in Uranium Dioxide", *J. Chem. Phys.* **29**[1], 151-158 (1958).
12. Y. Saito, "Nonstoichiometry in Uranium Dioxide", *J. Nucl. Mater.* **51**, 112-125 (1974).
13. A. M. Anthony, "Les Equlibres des Composes Oxygenes de l'uranium entre 1500 et 2000 K", *J. Nucl. Mater.* **10**[1], 8-14 (1963).
14. K. Nagarajan, R. Saha, R. B. Yadav, S. Rajagopalan, K. V. G. Kutty, M. Saibaba, P. R. V. Rao and C. K. Mathews, "Oxygen Potential Studies on Hypostoichiometric Uranium-cerium Mixed Oxide", *J Nucl. Mater.* **130**, 242-249 (1985).
15. W. Doerr, S. Hellmann, and G. Mages, "Study of the Formation of UO_2-PuO_2 Solid Solution by Means of UO_2-CeO_2 Simulate", *J. Nucl. Mater.* **140**, 7-10 (1986).
16 T. L Markin and E. C. Crouch, "Themodynamic data for U-Ce-Oxides", *J. Inorg. Nucl. Chem.* **32**, 77-82 (1970).
17. R. Ducroux and Ph. J. Baptiste, "Mesure du Potential D'oxygenene Dans le Systeme $U_{0.7}Ce_{0.3}O_{2-x}$ a l'aaide d'une Minisonde a Electrolyte Solide", *J. Nucl. Mater.* **97**, 333-336 (1981).
18. D. I. R. Norris and P. Kay, "Oxygen Potential and Lattice Parameter Measurements in $(U,Ce)O_{2-x}$", *J. Nucl. Mater.* **116**, 184-194 (1983).
19. T. Fujino, "Thermodynamics of Fluorite Type Solid Solutions Containing Plutonium, Lanthanide Elements or Alkaline Earth Metals in Uranium Dioxide Host Lattices," *J. Nucl Mater.* **154**, 14-24 (1988).
20. S. -H. Kang and H. -I. Yoo, "Nonstoichiometry (δ) of $(Mg_xFe_{1-x})_{3-\delta}O_4$ Ferrite spinel", *Solid State Ionics* **86-88**, 751-755 (1996).
21. S. -H. Kang and H. -I. Yoo, "Composition (x) Dependence of Nonstoichiometry (δ) in Ferrite Spinel $(Mg_xFe_{1-x})_{3-\delta}O_4$", in press.
22. B. T. M. Willis, "Structures of UO_2, UO_{2+x}, U_4O_9 by Neutron Diffraction," *J. Phys.* **25**[5], 431-439 (1964).
23. B. T. M. Willis, "The Defect Structure of Hyperstoichiometric Uranium Dioxide", *Acta. Cryst.* **A34**, 88-90 (1978).
24. H. S. Kim, Y. K. Yoon, Y. W. Lee, "Defect Structures of $(U_{1-y}Er_y)O_{2\pm x}$ Solid Solutions", *J. Nucl. Mater.* **226**, 206-215 (1995).
25. T. L. Markin and R. J. Bones, "Thermodynamics Data for Uranium Oxides between UO_2 and U_3O_8", Thermodyn. Nucl. Mater., Proc. Symp., Vienna 1962, pp. 693-710.
26. K. Hagemark and M. Broli, "Equilibrium Oxygen Pressures over Solid Solutions of Urania-yttria and Urania-lanthana at 1100° to 1400°C", *J. Am. Ceram. Soc.* **50**[11], 563-567 (1967).
27. K. Une and M. Oguma, "Oxygen Potential of $U_{0.96}Gd_{0.04}O_2$ (UO_2-3 wt% Gd_2O_3) Solid Solution", *J. Nucl. Mater.* **131**, 88-91 (1985).
28. T. B. Lindemer and A. L. Sutton, Jr., "Study of Nonstoichiometry of $<U_{1-y}Gd_yO_{2+x}>$", *J. Am. Ceram. Soc.* **71**[7], 553-561 (1988).
29. H. S. Kim, Y. K. Yoon, M. S. Yang, "Thermodynamic Study on the $(U_{1-y}Er_y)O_{2+x}$ Solid Solutions", *J Nucl. Mater.* **226**, 206-215 (1994).
30. S. -H. Kang, J -H. Lee, H. -I. Yoo, H. S. Kim and Y. W. Lee, "Measurement of Nonstoichiometry (x) of UO_{2+x} and $(Er_{0.08}U_{0.94})O_{2+x}$ by a Coulometric Titration Method", *J. Kor. Ceram. Soc.* **34**[7], 722-730 (1997).
31. P. Kofstad, in Nonstoichiometry, Diffusion and Electrical Conductivity in Binary Metal Oxides, pp. 276-278, John Wiley & Sons, Inc., New York, 1972.